PHOTOCATALYTIC DEGRADATION OF IRON CYANOCOMPLEXES BY TiO_2 BASED CATALYSTS

Rafael van Grieken *, José Aguado, María-José López-Muñoz and Javier Marugán

Department of Chemical, Environmental and Materials Technologies. ESCET.

Universidad Rey Juan Carlos. C/ Tulipán s/n, 28933 Móstoles, Madrid, Spain.

* E-mail: rafael.vangrieken@urjc.es Phone: +34 91 488 7007 Fax: +34 91 488 7068

Published on:

Applied Catalysis B: Environmental, 55:201-211 (2005).

doi:10.1016/j.apcatb.2004.08.008

Abstract

The removal of iron cyanocomplexes in industrial effluents is a difficult process, due to the resistance of these compounds to conventional treatments for cyanide wastewater detoxification. The mechanism of both the homogeneous photolysis of these compounds and their heterogeneous photocatalytic oxidation with Degussa P25 TiO_2 and silica-supported TiO_2 photocatalysts have been investigated. The activities of the tested catalysts for complexed cyanide degradation were found to be different from those observed for free cyanide photo-oxidation. The best activity was found for the photocatalyst synthesized by supporting 20 wt% of TiO_2 on SBA-15 silica as compared with the commercial catalyst Degussa P25 and the other supported catalysts tested. On the basis of detected intermediate species, a mechanism for iron cyanocomplexes photodegradation is suggested. The influence of the textural properties of the support and titania loading on the process is discussed. The results point out that the high activity observed when SBA-15 is used as support of TiO_2 seems to be related to the microporosity of the material acting as molecular sieve which avoids the deactivation of the semiconductor.

The porous structure of the SBA-15 material limits the access of the iron cyanocomplexes to the TiO_2 particles whereas the free cyanides homogeneously released can reach the semiconductor surface, being subsequently oxidized to cyanate.

Keywords

Photocatalysis; Supported-TiO_2; SBA-15; Cyanide; Cyanocomplexes; Ferricyanide; Ferrocyanide; Hexacyanoferrate.

1. Introduction.

Hexacyanoferrate (II) and (III) are some of the cyanide-containing species most commonly occurring in wastewater effluents of electroplating factories, gold mining tailings and coal gasification processes. Within the framework of environmental considerations, iron-complexed cyanides are usually considered in a first approximation as weakly toxic due to both the toxicity levels for various organisms [1,2] and the stability of their dilute solutions in the dark [3]. A further approach to the photochemistry of hexacyanoferrate (II) and (III) complexes reveals their potential hazard, mainly due to the fact that they can evolve by photolysis on exposure to light of proper energy in the UV-vis range releasing free cyanides, species of well known toxicity [3-6]. Experiments carried out by Meeussen *et al*. [7] showed that even diffuse daylight was able to produce decomposition of iron-cyanide complexes to free cyanide at a rate of 8 % hr^{-1}. Faster decomposition rates were reported by Marsman *et al*. [8] by exposing groundwater contaminated with iron-cyanide complex ions to UV-light. Taking into account that it is not unlikely that wastewater effluents containing iron (II) and (III) cyanocomplexes may be exposed to solar radiation, it is desirable to treat them before being discharged to the environment. This measure would avoid the risks leading to soil and groundwater contamination associated with these compounds.

The techniques commonly used for the treatment of industrial wastewater containing cyanide compounds include alkaline chlorination, and ozone or hydrogen peroxide oxidation [9,10]. Among them the chlorination procedure, a method originally patented in Germany in 1943, is the most widely used. However, although it is very effective for the degradation of free cyanides and a large variety of metal cyanocomplexes, this treatment does not readily work for iron cyanocomplexes mainly due to the low dissociation constants of these compounds. The ozone and hydrogen peroxide oxidation techniques are also unable to achieve an effective degradation of iron cyanocomplexes [10].

An attractive alternative to the procedures mentioned above is the use of Heterogeneous Photocatalysis, a technique which has shown its applicability for the

removal of either free [10-13] and iron-complexed cyanides [10,14-16]. There is general agreement that in the presence of titanium dioxide as photocatalyst, the oxidation of the iron-cyanocomplexes shows an initial release from the complex of free cyanides which are subsequently oxidized predominantly *via* a heterogeneous route to cyanate and nitrate species. The efficiency of the process, however, is not as high as it would be desirable for its application to wastewater treatment. For such purpose, further investigations are needed in order to elucidate the mechanism and nature of the intermediate species involved and to enhance the activity of the photocatalyst. In a previous work [16] we compared the activity of bare TiO_2 and different silica-supported TiO_2 samples for cyanides photodegradation. This work showed the influence of the silica support on the activity of the catalyst. Moreover, promising results for hexacyanoferrate (III) species photodegradation with a sample prepared supporting TiO_2 (20% wt loading) on mesostructured silica (SBA-15) were obtained in this preliminary study. On this basis, the present work has been devoted to investigate the mechanism of the photocatalytic-assisted oxidation of hexacyanoferrate (II) and (III) using a TiO_2 commercial sample and silica supported titania catalysts. The effect of titania loading and the influence exerted by the silica support on the titania activity have been investigated.

2. Experimental.

2.1. Catalysts Preparation

The synthesis of the supported titania samples has been described elsewhere [17]. It is based on the sol-gel hydrolysis of titanium isopropoxide in the presence of the chosen silica support, in the proper ratio to get the desired nominal titania content (20, 40 and 60 weight %). The resulting solid is hydrothermally treated at 170ºC and further calcinated at 550ºC. Two silica supports were tested: the mesostructured so-called SBA-15 silica [18] (B.E.T. specific surface area of 640 m^2g^{-1}) and a commercial amorphous silica (Grace Sylopol 2104, S_{BET} = 317 m^2g^{-1}) which will be referred to as GrS. Hereinafter, the catalysts will be named by indicating their nominal TiO_2 content,

followed by the silica support name, *e.g.* X% TiO_2/SBA-15 or GrS. The materials obtained upon supporting TiO_2 on SBA-15 presented specific surface areas of 532 m^2g^{-1} (20%TiO_2/SBA-15), 442 m^2g^{-1} (40%TiO_2/SBA-15), and 349 m^2g^{-1} (60%TiO_2/SBA-15). Their average TiO_2 crystal sizes were 6.2, 6.7, and 6.8 nm respectively. The sample 20%TiO_2/GrS presented a specific surface area of 299 m^2g^{-1}, and an average TiO_2 crystal size of 6.8 nm. Regardless of the chosen support, anatase was the only crystalline phase detected in the X-ray diffraction patterns of the samples.

Degussa P25 titanium dioxide, well known for its high activity in a great variety of photocatalytic reactions, was used as reference. It is a non-porous solid, with a B.E.T. surface area of 50 m^2g^{-1} and a mean particle size of *ca*. 30 nm. It contains both anatase and rutile crystalline phases in a ratio of 4:1.

2.2. Photoreaction runs procedure

The photoreaction runs were carried out in a cylindrical Pyrex batch reactor of 1 liter as effective solution volume, with two openings for withdrawing samples and bubbling of air. UV-irradiation of the reacting solution was performed with an immersed 150 W medium pressure mercury lamp (Heraeus TQ-150) placed inside a quartz jacket, and provided with a cooling tube for circulation of a cupper sulphate solution (0.02M) to prevent overheating of the reaction mixture and to remove the more energetic wavelengths (below 320 nm). The lamp was always switched on for 15 minutes before being fitted into the reactor, in order to achieve a stabilised radiation emission. In the meantime and throughout the overall experiment, air was bubbled in the reacting mixture made up from a reference cyanide solution and the amount of catalyst necessary to achieve a TiO_2 concentration of 0.5 g l^{-1}. The comparison of the tested catalysts was done at this fixed TiO_2 concentration because in our experimental conditions, only the semiconductor particles are expected to show photocatalytic activity.

Potassium cyanide (Aldrich, reagent grade), potassium hexacyanoferrate (II) and (III) (Scharlab, reagent grade) were used for the preparation of the reacting cyanide solutions, and NaOH (Scharlab, reagent grade) for adjusting their initial pH. In all the

experiments the initial concentration of either iron (II) or iron (III) hexacyanocomplex solutions was adjusted to the equivalent to 100 ppm of CN^- ions, assuming the release of six cyanide ions per molecule of iron complex. For this reason, unless stated otherwise, in all the Figures and throughout the subsequent results and discussion, the concentration of hexacyanoferrate (II), hexacyanoferrate (III) and cyanate ions are expressed in terms of CN^- ppm (*i.e.*, $[Fe(CN)_6]^{3-}$ 0.64 mM corresponds to a concentration of 100 ppm of CN^- ions; likewise, a 3.84 mM CNO^- solution would be equivalent to a 100 ppm CN^- ions).

During the reaction, which usually lasted for 4 or 6 hours, the reaction mixture was stirred constantly and kept at a temperature of 25 ± 1ºC. Aliquots were taken from the irradiated solutions at time intervals, following filtration through 0.22 μm Nylon membranes before being analysed.

2.3. Analytical procedure.

Free cyanide concentrations lower than 5 mg l^{-1} were determined using a standard colorimetric method [3]. The method is based on the initial conversion of CN^- to CNCl followed by the addition of a pyridine-barbituric acid reagent to develop a blue-red colour with maximum absorbance at 575 nm. The absorption measurements were performed with a Varian Cary 500 Scan UV-Vis-NIR spectrophotometer. Cyanide concentrations higher than 5 mg l^{-1}, were determined potentiometrically using a CN^--selective electrode in an expandable ion analyser (Orion 720A).

Identification and quantitative analysis of cyanate species were performed by ion chromatography in a Metrohm equipment (Separation centre 733, IC detector 732, Pump Unit 752). An aqueous solution of $NaHCO_3$ (2.0 mM) and Na_2CO_3 (1.3 mM) at a flow rate of 0.8 ml min^{-1} was used as eluent.

Determination of iron content in either solutions or solids was carried out by a Varian Vista AX inductive coupled plasma-atomic emission spectrometer (ICP-AES). Identification of the different complexed cyanide species involved in the reactions was performed by UV-vis absorption spectroscopy, following different methods as

explained below. Determination of $[Fe(CN)_6]^{3-}$ and/or $[Fe(CN)_6]^{4-}$ species in solution was made following a procedure developed in our laboratory, based in the ISO 7766-1:1993 method [19]. The standard method allows the analysis of both iron hexacyanocomplexes through the blue colour development (Prussian blue) in the solution upon addition of ferrous and ferric reagents, and the subsequent measurement of the absorbance at 700 nm [19]. Distinction between the hexacyanoferrate (II) and (III) complexes was performed by a first addition of the ferric reagent, which reacts selectively with $[Fe(CN)_6]^{4-}$. Hexacyanoferrate (III) species can be determined by difference from the results obtained upon addition of the ferrous reagent, as it induces the blue colour development in the presence of any of either Fe(II) or Fe (III) hexacyanocomplexes. Identification of hydroxopentacyanoferrate (III) and aquapentacyanoferrate (III) was made through the analysis of the UV-Vis spectra of the solutions. As compared to the hexacyanoferrate (III) complex, which presents an absorption maximum at 420 nm, a blue shift to 400 nm is observed upon substitution of one CN^- ligand for H_2O or OH^- [5]. Analysis for aquapentanocyanoferrate (II) was performed by its reaction with nitrosobenzene [20], which yields an intensively coloured complex $[Fe(CN)_5(C_6H_5NO)]^{3-}$. The latter shows in its visible spectrum an absorption maximum at 528 nm, for which an extinction coefficient value of 5300 dm^3 M^{-1} cm^{-1} has been reported [21]. Although these analytical methods provide quantitative data for the different iron cyanocomplexes present in the solution, the aim of the work was to establish the photodegradation mechanism without a rigorous kinetic modelling.

3. Results.

3.1. Homogeneous photodegradation of hexacyanoferrate (III) and (II).

The influence of the initial pH of the reacting solution in the homogeneous photodegradation of the $[Fe(CN)_6]^{3-}$ species was initially studied. Figure 1 shows the results obtained at initial pH values of 10.5, 11.0, 12.0, and 13.0, respectively. Complexed-cyanide concentration was determined by a mass balance on nitrogen, defined as the difference between the initial hexacyanoferrate (III) amount and the concentration of CN^- and CNO^- species measured in the reaction mixture (neither

nitrate nor nitrite were detected). It is worth mentioning that the species named as "complexed cyanides" along the reaction run include not only $[Fe(CN)_6]^{3-}$ species but iron complexes where CN^- ligands may be substituted for either H_2O and/or OH^- ligands as discussed later on. The results obtained were checked and agreed with the amount of soluble iron species determined by ICP-AES. As it can be seen in Figure 1, whereas CN^- ions were detected in the solution under all experimental conditions used, thus confirming the homogeneous release of free cyanides from the complex, production of cyanate ions was shown to be highly dependent on the initial pH of the solution. From Figure 1, the highest formation of the oxidation product was achieved at initial pH values within the range (11.0-12.0) whereas the release of free cyanides stepped up as the initial pH of the solution was increased from 10.5 to 13.0. Concomitantly to the CN^- release from the complex as the irradiation proceeded, it was observed the formation of a reddish brown precipitate. For equal irradiation times, the amount of solid recovered after the reaction was higher as the initial pH value of the solution increased. The analysis of the solid by ICP-AES confirmed an iron content attributable to $Fe(OH)_3$ species, which is in agreement with the finding of Augugliaro *et al.* [14] and Rader *et al.* [15].

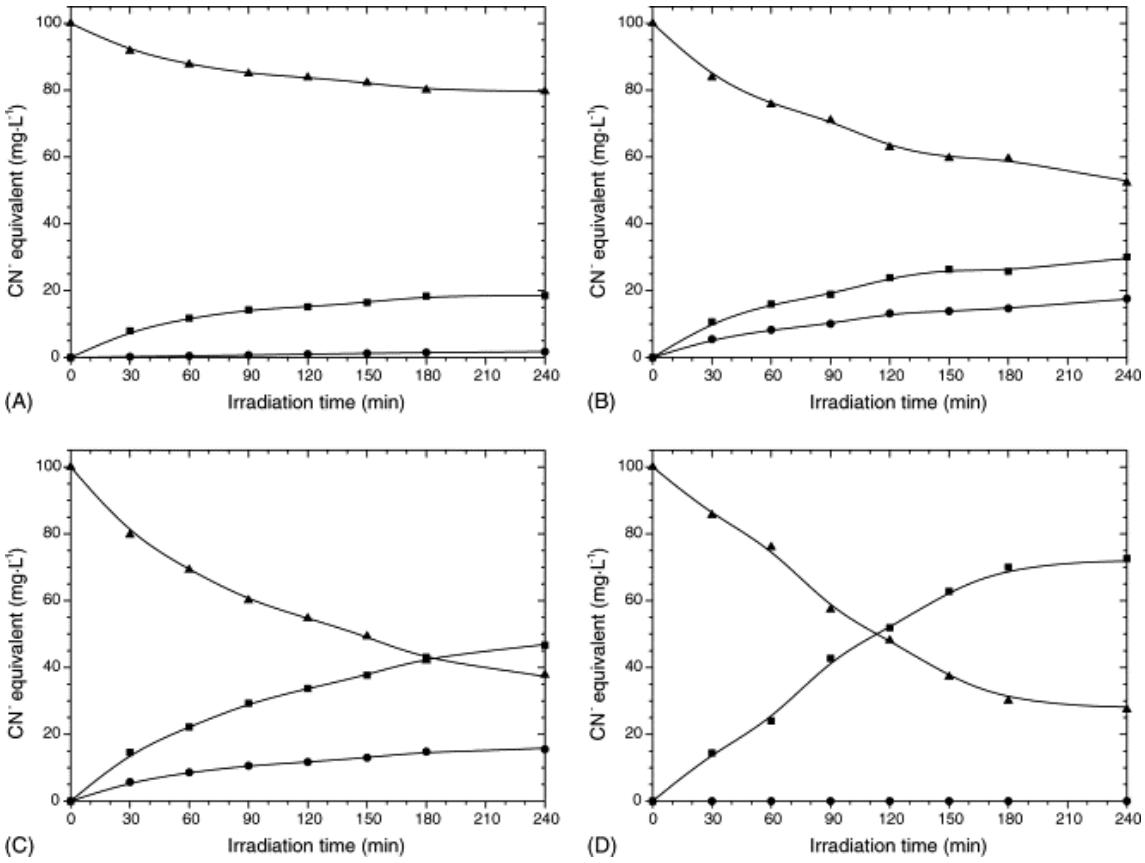

Figure 1. Homogeneous photodegradation of hexacyanoferrate (III) at initial pH = 10.5 (A), pH = 11.0 (B), pH = 12.0 (C) and pH = 13.0 (D). (▲ Complexed-cyanide, ■ Free Cyanide, ● Cyanate).

In order to get information on the nature of intermediate products derived from the homogeneous irradiation of hexacyanoferrate (III) ions, the analytical reaction tests previously described in the Experimental section were carried out. The UV-vis spectra showed a fast decay of the absorption maximum at 420 nm attributed to $[Fe(CN)_6]^{3-}$ species, together to its subsequent blue shift to 400 nm indicative of the presence of hydroxopentacyanoferrate (III) and/or aquapentacyanoferrate (III) complexes [5]. Following increasing irradiation times, the absorbance at 400 nm increased to a maximum value after which it decreased. In none of the runs $[Fe(CN)_6]^{4-}$ species were detected. Reaction of the solutions with nitrosobenzene to analyze the formation of $[Fe(CN)_5(H_2O)]^{3-}$ species, resulted in the expected colour development. However, it was not achieved immediately upon the reagent addition but several minutes later. This delayed colour development, was also observed by Fuller *et al*. [5], who attributed it to

the formation of bisferrate dimeric species $[Fe_2(CN)_{10}]^{6-}$ whose slow decomposition may be the cause of such slow colour development. Therefore, although it can be discarded a significant photo-induced iron reduction of the hexacyanoferrate (III) complex to yield the hexacyanoferrate (II) complex, at a certain stage of the reaction some redox processes leading to the formation of iron (II) derived species must take place.

During the reaction runs, the pH of the solutions was monitored. A significant pH drop down to 8.8 was observed in the experiment in which the initial pH had been adjusted to 10.5. Taking into account the pK_a value of hydrogen cyanide (9.2), cyanide ions released from the complex under the irradiation may yield highly toxic HCN. On this basis, such initial pH must be discarded in the treatment of hexacyanoferrate (III) solutions that may be exposed to either artificial-UV radiation or direct sunlight. Initial pH value of 13.0 was also discarded for the following experiments because at such high pH some silica dissolution could be induced from either the supported catalysts or the Pyrex reactor.

Substantially different results were observed in the corresponding trials of homogeneous irradiation of hexacyanoferrate (II) solutions. Figure 2 shows the reaction profiles obtained in two runs in which the initial pH was fixed at 11.0 and 12.0 respectively. The absence of oxidation products such as cyanate ions is noticeable in contrast to the analogous experiments carried out with the iron (III) hexacyanocomplex. The test for $[Fe(CN)_6]^{3-}$ detection was negative in all aliquots thus indicating the photoinduced degradation of the hexacyanoferrate (II) solutions does not proceed through a photo-oxidation of the iron atom in the hexacyanocomplex. The quick formation of the intensively coloured $[Fe(CN)_5(C_6H_5NO)]^{3-}$ complex upon addition of nitrosobenzene to the reaction aliquots, probed the formation of aquapentacyanoferrate (II) species during the runs. The final oxidation state of iron ions deriving from the hexacyanoferrate (II) is however (3+), as expected in the alkaline conditions, according to the formation along the reaction of increasing amounts of the reddish precipitate attributable to $Fe(OH)_3$, in a similar way to that observed following irradiation of hexacyanoferrate (III) solutions.

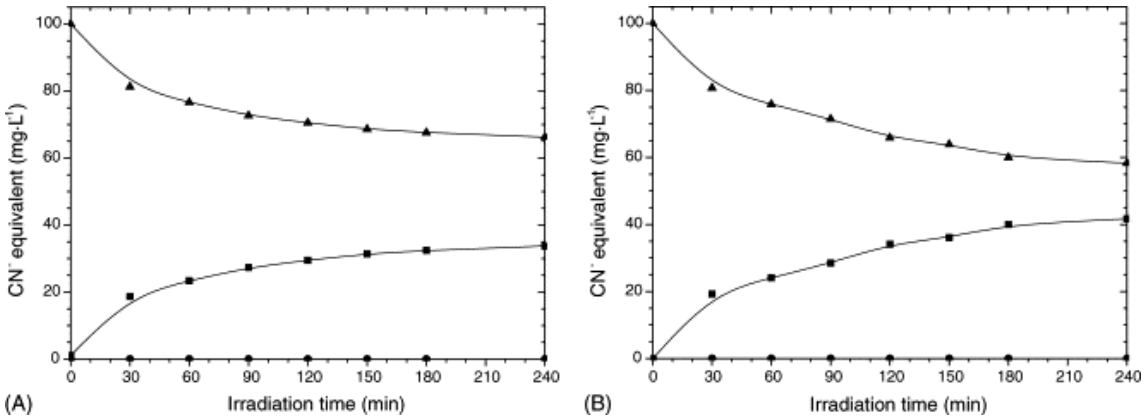

Figure 2. Homogeneous photodegradation of hexacyanoferrate (II) at initial pH = 11.0 (A) and pH = 12.0 (B). (▲ Complexed-cyanide, ■ Free Cyanide, ● Cyanate).

3.2. Heterogeneous photodegradation of hexacyanoferrate (III) and (II) with Degussa P25 TiO_2.

Figure 3 shows the reaction profiles obtained during the irradiation of hexacyanoferrate (III) solutions in the presence and in the absence of TiO_2 (Degussa P25 sample) at initial pH values of 11.0 and 12.0. As compared with the homogeneous reactions performed at the same initial pH values (dashed lines in Figure 3), the use of the commercial titania as catalyst caused a substantial decrease in the $[Fe(CN)_6]^{3-}$ degradation efficiency mainly at pH = 11.0. Moreover, it can be observed that at pH 12.0, the presence of the titania particles significantly enhanced the ratio of cyanide to cyanate species found in the solution. UV-vis spectroscopy analytical tests for identifying the intermediate iron-containing species in solution probed the formation of the hydroxopentacyanoferrate (III) and/or aquapentacyanoferrate (III) complexes. Furthermore, the formation of a significant concentration of hexacyanoferrate (II) species was evidenced through Prussian blue development whereas the reaction with nitrosobenzene reagent probed the presence of $[Fe(CN)_5(H_2O)]^{3-}$ species in the solution. Such Fe(II)-containing complexes indicated that, not only the substitution of the cyanide ligands in the initial $[Fe(CN)_6]^{3-}$ complex, but reduction of the complexed iron takes place in the presence of the titania catalyst.

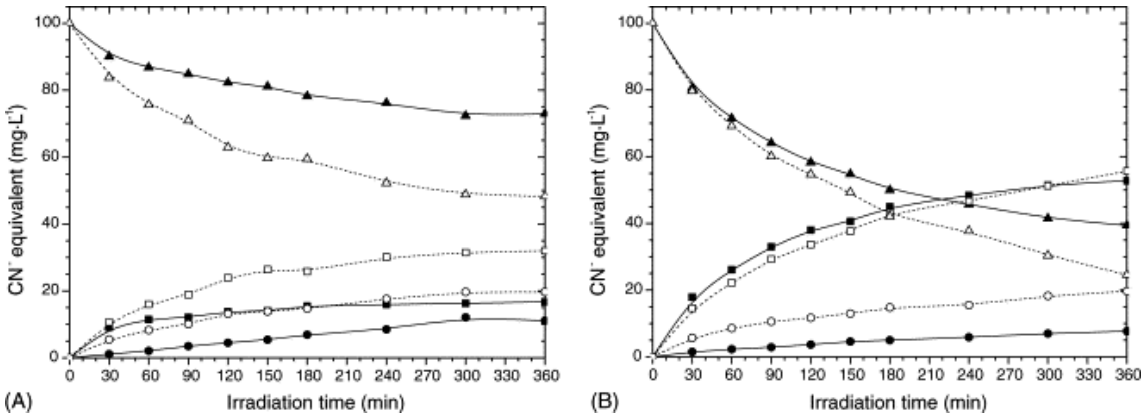

Figure 3. Heterogeneous photodegradation of hexacyanoferrate (III) with Degussa P25 TiO_2 at initial pH = 11.0 (A) and pH = 12.0 (B). (▲ Complexed-cyanide (heterogeneous), ■ Free Cyanide (heterogeneous), ● Cyanate (heterogeneous), △ Complexed-cyanide (homogeneous), □ Free Cyanide (homogeneous), ○ Cyanate(homogeneous)).

Once the reaction was concluded, the catalyst recovered by filtration showed a reddish-brown colour indicative of $Fe(OH)_3$ formation.

An activity trend similar to that shown for the hexacyanoferrate (III) species was obtained in the experiments carried out with ferrocyanide solutions. Figure 4 shows the reaction profiles obtained following the photodegradation of the hexacyanoferrate (II) solution in the presence of Degussa P25 TiO_2 at initial pH value of 12.0. In comparison with the homogeneous process carried out at the same initial pH value (discontinuous lines in figure 4), UV-irradiation in the presence of the commercial catalyst showed more efficiency for the Fe (II)-complex degradation not only concerning the release of free cyanides, but also for cyanate ions formation. Moreover, analytical tests for the determination of intermediate species also showed other meaningful differences. Besides the formation of aqua- and/or hydroxopentacyanoferrate (II) species, significant amounts of hexacyanoferrate (III), aqua- and/or hydroxopentacyanoferrate (III) species were produced during the irradiation in the presence of TiO_2 thus implying redox processes induced by the catalyst.

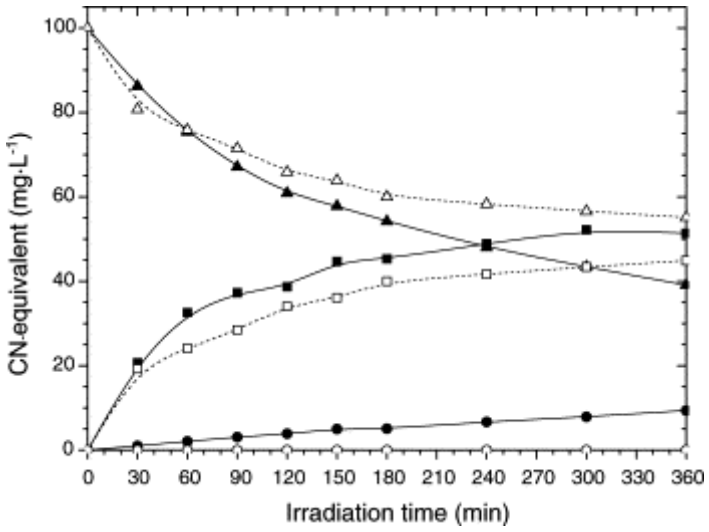

Figure 4. Heterogeneous photodegradation of hexacyanoferrate (II) solution with Degussa P25 at initial pH = 12.0. (▲ Complexed-cyanide (heterogeneous), ■ Free Cyanide (heterogeneous), ● Cyanate (heterogeneous), △ Complexed-cyanide (homogeneous), □ Free Cyanide (homogeneous), ○ Cyanate(homogeneous)).

3.3. Heterogeneous photodegradation of hexacyanoferrate (III) and (II) with 20%TiO_2/SBA-15 catalyst.

Figures 5 and 6 show the reaction patterns obtained upon UV-irradiation of hexacyanoferrate (III) and (II) solutions in the presence of 20%TiO_2/SBA-15 material. As compared with either the homogeneous experiments or those performed with Degussa P25 TiO_2 catalyst, a remarkably high efficiency is exhibited by this supported catalyst for the oxidation of the CN^- ions released from the complex. As a consequence, concentration of free cyanide ions was low in the solution during the reaction whereas increasing CNO^- amounts were detected in both iron (II) and (III) hexacyanocomplexes solutions.

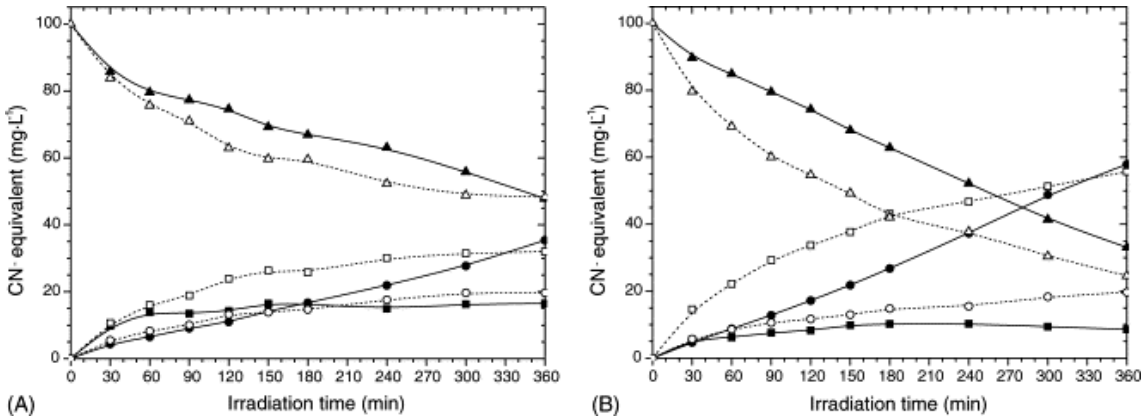

Figure 5. Heterogeneous photodegradation of hexacyanoferrate (III) solutions with 20%TiO_2/SBA-15 at initial pH values of 11.0 (A) and 12.0 (B). (▲ Complexed-cyanide (heterogeneous), ■ Free Cyanide (heterogeneous), ● Cyanate (heterogeneous), △ Complexed-cyanide (homogeneous), □ Free Cyanide (homogeneous), ○ Cyanate(homogeneous)).

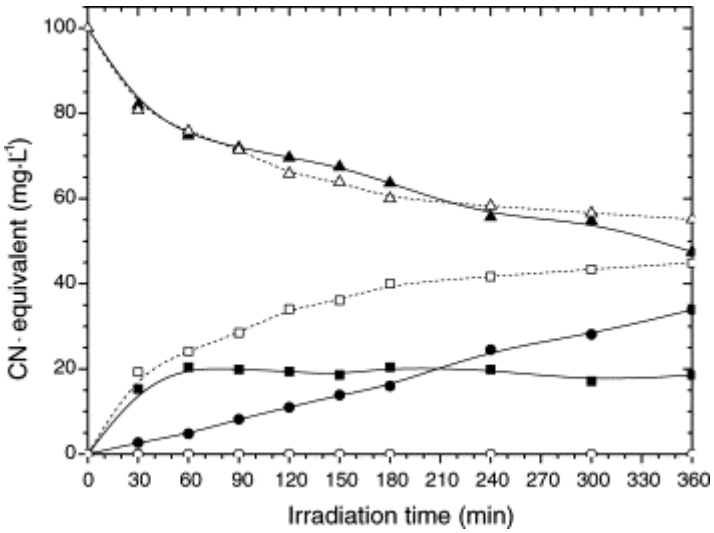

Figure 6. Heterogeneous photodegradation of a hexacyanoferrate (II) solution with 20%TiO_2/SBA-15 at initial pH value of 12.0. (▲ Complexed-cyanide (heterogeneous), ■ Free Cyanide (heterogeneous), ● Cyanate (heterogeneous), △ Complexed-cyanide (homogeneous), □ Free Cyanide (homogeneous), ○ Cyanate(homogeneous)).

The analysis of the products formed along the reaction suggested some changes in the reaction pathway brought about by the supported TiO_2 in comparison to the bare TiO_2 catalyst. It was observed in the case of $[Fe(CN)_6]^{3-}$ degradation that, in contrast to the results obtained with the Degussa P25 TiO_2, $[Fe(CN)_6]^{4-}$ and $[Fe(CN)_5(H_2O)]^{3-}$ were only scarcely detected during the reaction. Similarly, the experiments performed with $[Fe(CN)_6]^{-4}$ solutions showed insignificant formation of $[Fe(CN)_6]^{3-}$ and $[Fe(CN)_5(H_2O)]^{-2}$ products along the irradiation of the system.

It is worth mentioning that in the presence of the 20%TiO_2/SBA-15 catalyst, in no case the reddish colour indicative of $Fe(OH)_3$ formation was observed. In fact, once the reaction had been concluded, the catalyst recovered upon filtration appeared completely white and the remaining solution was colourless. The analysis of the solid performed by means of ICP-AES spectroscopy revealed an iron content in accordance to the amount expected from the CN^- and CNO^- concentrations measured in solution. Such iron value was calculated by considering that the degradation of each iron hexacyanocomplex molecule yields one iron atom and six cyanide equivalent species.

3.4. Influence of the TiO_2 content and type of silica in the supported catalysts.

The effect of increasing titania loading on the SBA-15 silica support was evaluated by testing the activity of the 40%TiO_2/SBA-15 and 60%TiO_2/SBA-15 samples for hexacyanoferrate (III) photodegradation. The cyanide distribution after 6 h irradiation is shown in Figure 7. As the percentage of titania content was increased, the efficiency of the catalysts for further oxidation of CN^- ions released from the complex diminished. The influence of the silica support was also studied by performing experiments using a non-structured silica (20%TiO_2/GrS sample) and a sample prepared by physical mixture of Degussa P25 TiO_2 with the mesostructured silica (SBA-15) in the proper ratio to get a 20% wt. content in TiO_2 (Figure 7). The low conversion of released cyanide ions to cyanate species achieved with the latter samples as compared with the 20%TiO_2/SBA-15, clearly indicates the importance not only of the silica morphology but of the specific interaction taking place between the titania particles and the support.

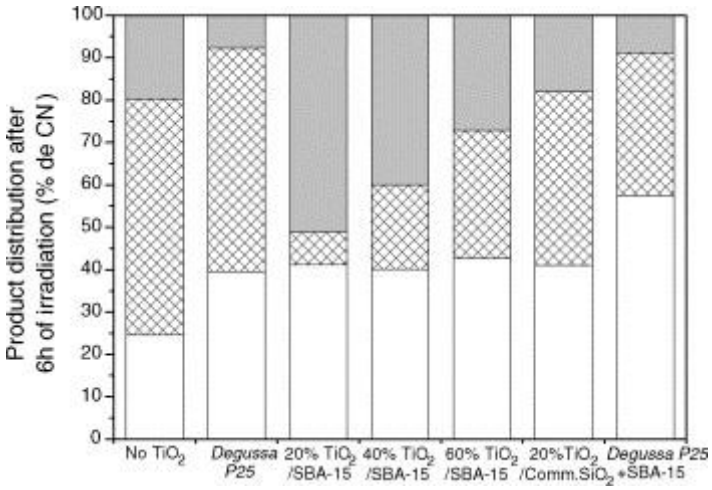

Figure 7. Comparison of products distribution obtained upon UV-irradiation of hexacyanoferrate (III) solutions in the presence of different catalysts. (☐ Complexed-cyanide, ☒ Free Cyanide, ▩ Cyanate)

After finishing the reaction the catalysts were recovered by filtration of the suspensions. Unlike the Degussa P25 TiO_2 sample, all the silica-containing samples, e.g. 20%TiO_2/SBA-15, 40%TiO_2/SBA-15, 60%TiO_2/SBA-15, 20%TiO_2/GrS samples and the (P25+SBA-15) mixture showed no colour attributable to $Fe(OH)_3$ deposition. Nevertheless, ICP-AES analysis of the solids confirmed in each case an iron content matching with the measured CN^- and CNO^- concentrations in the solutions, as explained before. Consequently, the apparent inhibition of $Fe(OH)_3$ formation is not restricted to the 20%TiO_2/SBA-15 catalyst but to all the other containing silica samples tested.

3.5. Heterogeneous photodegradation of free cyanides and iron cyanocomplexes mixtures.

Finally, the influence of the presence of free cyanides in the hexacyanoferrate (III) photocatalytic degradation was investigated. A reaction mixture made up of 50 ppm of free CN^- ions provided from potassium cyanide and 50 ppm of complexed CN^- ions as hexacyanoferrate (III) species was used to evaluate the catalysts performance.

Figure 8 shows the results obtained upon UV-irradiation of the solution in the presence of either Degussa P25 TiO_2 or 20%TiO_2/SBA-15 catalysts at initial pH value of 12.0.

Figure 8 shows a lower activity for cyanide ions oxidation in the case of Degussa P25 sample as compared with the 20%TiO_2/SBA-15 sample. Whereas the use of the supported titania allowed to achieve the oxidation of most of CN^- ions initially present in the solution, a steady cyanide concentration, similar to the initial one, was observed to remain during the reaction performed in the presence of Degussa P25 TiO_2.

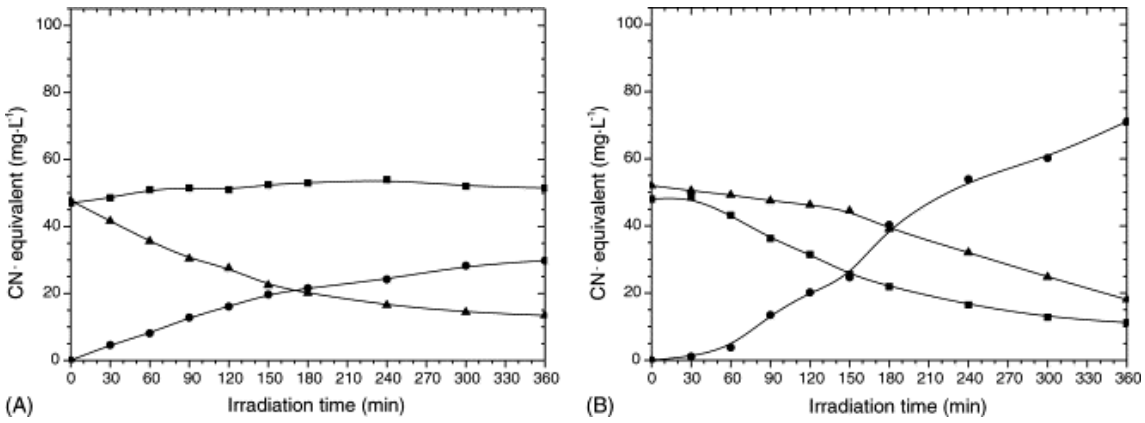

Figure 8. Heterogeneous photodegradation of free cyanides and hexacyanoferrate (III) mixtures at initial pH value of 12.0 with Degussa P25 (A) and 20%TiO_2/SBA-15 (B). (▲ Complexed-cyanide, ■ Free Cyanide, ● Cyanate).

4. Discussion

4.1. Homogeneous photodegradation of hexacyanoferrate (II) and (III) complexes

Photochemistry of metal cyanocomplexes has been extensively studied by many authors [22 and references included]. Hexacyano homoleptic complexes are known to undergo photosubstitution of a cyanide ligand forming mixed-ligand cyanides, and this has been proposed as one of the primary photochemical steps that take place upon UV-irradiation of their solutions:

$$[M(CN)_6]^{m-} + L \rightarrow [M(CN)_5L]^{1-m} + CN^- \qquad (1)$$

Not only cyanide ion but ligand L photosubstitution can occur in those mixed-ligand cyanides complexes generated as it is stated above:

$$[M(CN)_5L]^{1-m} + L' \rightarrow [M(CN)_5L']^{1-m} + L \qquad (2)$$

In the case of Fe (II) and Fe (III) cyanocomplexes, as H_2O and OH^- are the only ligands available for cyanide photosubstitution when their alkaline aqueous solutions are irradiated, formation of iron aquapentacyano and/or iron hydroxopentacyano species should be expected, together to the subsequent release of cyanides ions. Although there is general agreement in considering these processes as the primary steps, many questions concerning the mechanism of the iron cyanocomplexes photodegradation such as the fate of the released cyanide ions and the intermediary species formed are, however, not solved nowadays.

As described in the Results, irradiation of hexacyanoferrate (III) solutions leads to a decay and blue shift of the absorption maximum initially centred at 420 nm to 400 nm in their UV-vis spectra. According to the UV-vis spectra reported by Fuller *et al.* [5], the absorption maxima of the aquapentacyanoferrate (III) and hydroxopentacyanoferrate (III) species overlap at a wavelength of *ca.* 400 nm, but the extinction coefficient value of $[Fe(CN)_5(OH)]^{3-}$ species is much higher than of $[Fe(CN)_5(H_2O)]^{2-}$ species. We observed that once the maximum at 400 nm is formed, further irradiation of the system resulted in a subsequent increase of the absorbance at that wavelength until reaching a maximum value, which afterwards decreased as the reaction proceeded. On this basis, our results confirm a mechanism in which a preliminary photoaquation of the hexacyanoferrate (III) complex takes place to form the aquapentacyanoferrate (III) as primary species:

$$[Fe(CN)_6]^{3-} + H_2O \leftrightarrow [Fe(CN)_5(H_2O)]^{2-} + CN^- \qquad (3)$$

The photosolvation step must be followed by the H_2O ligand substitution for hydroxyl groups to form $[Fe(CN)_5(OH)]^{3-}$ species, in a process highly dependent on the pH value, thus explaining the increase in intensity of the absorption maximum centred at 400 nm. A further substitution of remaining cyanide ligands by hydroxyl groups and/or water molecules must continue up to the precipitation of $Fe(OH)_3$ through irreversible

reactions. The global stoichometric reaction can be then represented as a non-redox process leading to the release of free cyanide ions:

$$Fe(CN)_6^{3-} + 3\ OH^- \rightarrow Fe(OH)_3\downarrow + 6\ CN^- \qquad (4)$$

As the amount of hydroxyl groups available for ligand interchange in the complex increases, a more effective liberation of CN^- ions to the solution must be expected, as it is detected by increasing the initial pH of the solution from 10.5 to 13.0.

In the case of the hexacyanoferrate (II) complex, the formation of the aquapentacyanoferrate (II) species confirms the cyanide photosubstitution as primary step of the process, whereas the absence of $[Fe(CN)_6]^{3-}$ and other oxidation products leads to discard a photo-oxidation of the iron atom in the complex. Detection of $[Fe(CN)_5(H_2O)]^{3-}$ was also reported by Shirom and Stein [6] in experiments where UV-irradiation of ferrocyanide ion in aqueous solutions was performed over a pH range of 3.8-10.5. According to the reaction scheme proposed by these authors to explain the photochemistry of ferrocyanide ion in aqueous solution, the excited level to which is promoted $[Fe(CN)_6]^{4-}$ upon irradiation determines either its photoaquation or its oxidation with hydrated electron formation.

Regarding the fate of the released cyanide ions from both iron hexacyano complexes, our results show that their oxidation to yield cyanate species does not increase concomitantly to the rise of the cyanide concentration in the solution. In fact, the oxidation is completely inhibited at an initial pH value of 13.0, experimental conditions for which the highest CN^- liberation from the hexacyanoferrate (III) complex is achieved. Moreover, no cyanate ions were detected in any of the homogeneous irradiation experiments carried out with the hexacyanoferrate (II) complex in spite of the significant release of CN^- ions achieved. Independently of the nature of the complexes initially present in the solution ($[Fe(CN)_6]^{-3}$or $[Fe(CN)_6]^{-4}$) the CN^-/OCN^- couple should show the same redox potential in those experiments performed at the same initial pH values. Therefore, the differences found for both Fe(II) and Fe(III) systems must be due to the distinct oxidant species formed due to the irradiation in each case. Among the likely agents responsible for the homogeneous photo-oxidation

processes, singlet oxygen has been previously proposed [14]. In our system, it must initially be discarded, as the photon energy of the medium pressure mercury lamp used in these runs is not suitable for promoting the photoexcitation of molecular oxygen to the singlet state. Our experimental results point out to soluble iron (III) species as the main oxidizing agents in the homogeneous iron cyanocomplexes photodegradation, in agreement with the hypothesis of Rader et al. [15]. The absence of cyanate species in the experiments performed with the ferricyanide solutions at the highest pH values can then be explained in terms of a substantial decrease of those soluble Fe(III)-containing oxidising species, due to the more favoured process of $Fe(OH)_3$ precipitation. On the other hand, it would also be explained by the fact that no cyanide photo-oxidation takes place during the irradiation of hexacyanoferrate (II) solutions, independently of the initial pH value. As for the nature of such iron (III) oxidizing agents, the detection of the dimeric $[Fe^{II}_2(CN)_{10}]^{6-}$ ions upon the irradiation of hexacyanoferrate (III) solutions points out the $[Fe^{III}(CN)_5(H_2O)]^{2-}$ ions as plausible oxidant species through the following reaction:

$$2\,[Fe^{III}(CN)_5(H_2O)]^{2-} + CN^- \rightarrow [Fe^{II}_2(CN)_{10}]^{6-} + OCN^- + H_2O + 2\,H^+ \qquad (3)$$

According to the results obtained upon irradiation of the homogenous systems the following conclusions can be drawn. Even though the breakage of the hexacyanoferrate (II) complex under UV radiation takes place to a somehow lesser extent than the hexacyanoferrate (III) species, a substantial amount of cyanide ions are released to the solution in both cases. By lowering the pH of the system within a safety limit, according to the pK_a value of HCN, it is possible to reduce such cyanide release although it cannot be avoided in any case. As no common intermediates were formed, it can be concluded that the homogeneous photodegradation of iron hexacyanocomplexes follows a different route depending on the oxidation state of iron in the complex, so that there is no interlinked pattern between both complexed Fe (II) and Fe (III) systems. On the basis of the above considerations, the scheme shown in Figure 9 describes roughly the homogeneous photodegradation of both iron hexacyanocomplexes.

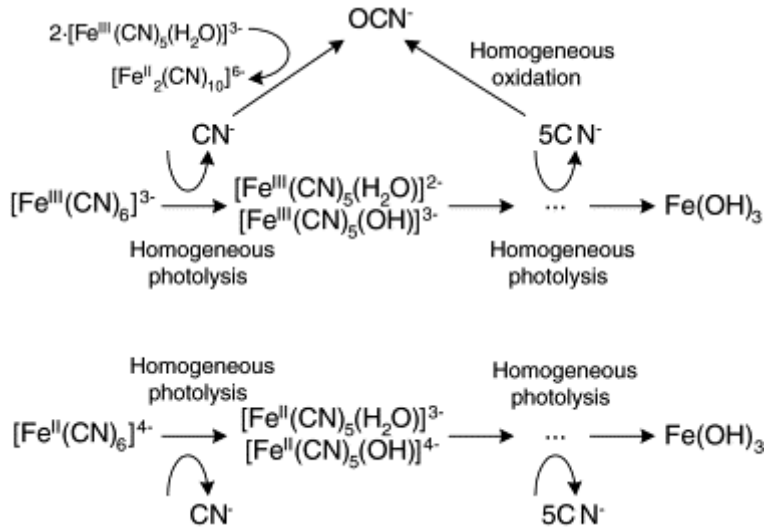

Figure 9. Mechanism of the homogeneous photodegradation of hexacyanoferrate (II) and (III) in solution.

4.2. Heterogeneous photodegradation of hexacyanoferrate (II) and (III) complexes.

The activity results obtained upon UV-irradiation of hexacyanoferrate (II) and (III) solutions in the presence of both Degussa P25 TiO_2 and 20%TiO_2/SBA-15 showed, as compared to the analogous homogeneous runs, different reaction patterns induced by the presence of the catalysts. If we limit our considerations just to the overall photodegradation of the hexacyano complex and not to the kind of products formed, the suspended catalyst particles had a detrimental effect in the case of the hexacyanoferrate (III) complex if compared with the results obtained in the homogeneous runs. This effect is specially remarkable with the Degussa P25 catalyst at an initial pH of 11.0 as shown in Figure 3. On the contrary, for hexacyanoferrate (II) photodegradation, the presence of TiO_2 Degussa P25 was even favourable. The reduction in activity for the hexacyanoferrate (III) photodegradation occurring in the heterogeneous system was also observed by Augugliaro *et al.* [14]. They attributed the detrimental effect of the TiO_2 particles to a decrease in the photon absorption by the reacting solution. It has been proposed [14,15] that iron cyanocomplexes photodegradation proceeds through both homogeneous and heterogeneous processes operating simultaneously. This mechanism implies an initial release of cyanides through a homogeneous process followed by their

heterogeneous oxidation. If the limiting step for the process is the homogenous breakage of the complex, the most effective initial decomposition of the iron hexacyanocomplex should take place in the absence of catalyst. The overall detrimental effect observed with both, the supported and bare TiO_2 catalysts might be therefore explained in terms of a competition between the iron (III) complex and the semiconductor for the photons provided to the system. Following this reasoning the same behaviour should be expected upon the irradiation of hexacyanoferrate (II) solutions in the presence of TiO_2 P25, as equal experimental conditions (e.g. radiant energy, catalyst and complex concentrations) were used. The better results obtained in the heterogeneous runs for the Fe (II) complex, not only in terms of the overall degradation but also for released cyanides oxidation points to a beneficial interaction between the complex and the catalyst. A plausible explanation should be that in the presence of TiO_2, intermolecular photo-oxidation of $[Fe(CN)_6]^{4-}$ or $[Fe(CN)_5H_2O]^{4-}$ takes place [22]. The adsorption of the iron (II) complex on the semiconductor may favour its behaviour as a quencher. The process would lead to the production of solvated electrons that can be injected in the conduction band of the semiconductor, with the subsequent oxidation of the iron in the complex. This would explain the detection of $[Fe(CN)_6]^{3-}$ in the solution and the very similar reaction patterns in terms of complex overall degradation, CN^- release and CNO^- production observed upon irradiation of either $[Fe(CN)_6]^{3-}$ or $[Fe(CN)_6]^{4-}$ in the presence of P25 TiO_2 at pH 12. According to these results, the diagram shown in Figure 10 might represent the mechanism of the heterogeneous photocatalytic degradation of both hexacyanocomplexes. In addition to the homogeneous degradation of the complexes, the presence of the catalyst induces the heterogeneous photo-oxidation of the released cyanide ions. The catalyst also links both complexes photodegradation processes through the redox reactions involving the different iron species, which take place on the semiconductor surface. As an example, the redox potential of the couple $[Fe(CN)]^{3-}$ /$[Fe(CN)]^{4-}$ is E_0 = 0.356 V [23], which is within the domain of the redox potentials of the photogenerated electron/hole pairs. The extension of the latter reaction depends on the catalyst nature. It is enhanced by using powdered bare TiO_2 in detriment of cyanate production, as the experimental results with Degussa P25 show. In contrast, in the presence of the 20%TiO_2/SBA-15 catalyst the extent of these redox processes involving

iron species is much lower but, on the other hand, it is the latter catalyst that shows a remarkably higher activity for cyanide oxidation to cyanate with both iron hexacyanocomplexes.

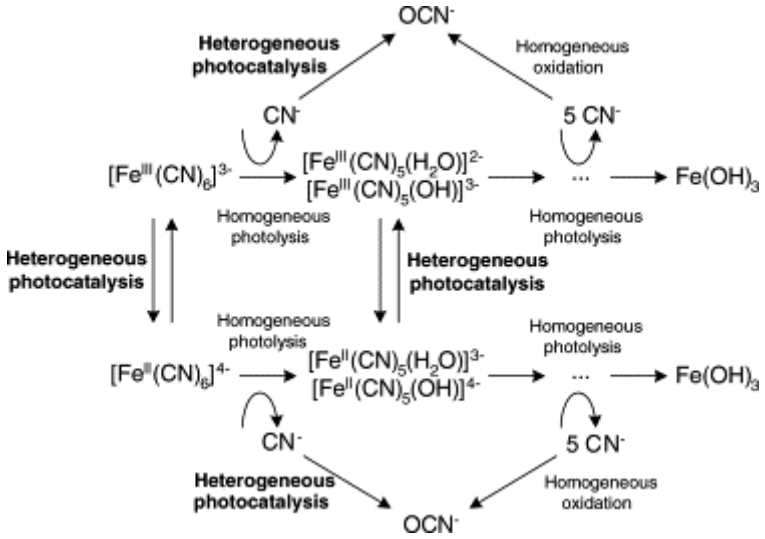

Figure 10. Mechanism of the heterogeneous photocatalytic degradation of hexacyanoferrate (II) and (III).

Considering the higher activity showed by the catalyst Degussa P25 for free cyanides photo-oxidation in comparison with the supported photocatalysts [16,17], the results point out the existence of a deactivating phenomenon of the semiconductor induced by the presence of the iron containing species derived from the degraded complexes. This fact is entirely confirmed by the results obtained for the photodegradation of mixtures of free cyanides and iron cyanocomplexes, showing that the presence of the iron species induces a much slower oxidation of the free cyanide ions. The deposition of $Fe(OH)_3$ over the semiconductor surface has been proposed by Rader et al. [15] as responsible for the deactivation of the bare TiO_2 catalyst. The results presented in this work show that in contrast to the bare TiO_2 catalyst, a higher cyanate to cyanide ratio was achieved with all the samples prepared by supporting the semiconductor on silica support. Moreover, none of the latter catalysts showed a coloration attributable to $Fe(OH)_3$ at the end of the reactions despite the analysis of

these catalysts confirmed the expected iron content (e.g. one iron atom for each six cyanide equivalent species detected). The great adsorption capability of iron ions on silica surface in aqueous solutions has been previously studied by different authors [24, 25]. Interaction between iron ions and surface hydroxyl groups on the silica surface can be proposed. The affinity between the metal ions and the SiO_2 surface can be considered as responsible of the beneficial effect of the silica in the iron cyanocomplexes photodegradation reactions, as it must reduce the accumulation of $Fe(OH)_3$ on the TiO_2 surface responsible of the deactivation semiconductor.

Although regeneration of the catalysts after the reaction seems to be possible by washing the materials at acidic pH (in which the iron hydroxide becomes soluble), further investigations are currently done in order to determine the influence of the iron deposits on the reutilization of the supported photocatalysts and to asses the possible decrease of the activity after several runs of reutilization of these materials.

Moreover, if we compare the results obtained with the 20%TiO_2/SBA-15 and the 20%TiO_2/GrS catalysts it is clear that not only the presence of the silica but its specific structural properties is crucial for the catalysts activity. The enhanced photoactivity for released cyanides oxidation observed for the TiO_2/SBA-15 photocatalysts if compared with either bare TiO_2 or TiO_2 supported on a non-structured silica, might probably be explained by taking into account the internal structure of the silica support. In addition to the mesoporous channels, the SBA-15 silica presents perpendicular micropores interconnecting them [26,27]. The synthesis procedure of the TiO_2/SBA-15 materials is based on the controlled growth of the TiO_2 clusters inside the mesoporous channels of the silica. Such channel structure might avoid the deactivation of the semiconductor by limiting the access of the iron cyanocomplexes to the TiO_2 surface. By contrast, the free cyanides homogeneously released can reach the semiconductor surface, being subsequently oxidized to cyanate. This hypothesis is supported by the size of the molecules estimated with Cerius^2 software (Molecular Simulations Inc.), 3.356 Å and 9.449 Å for CN^- and $[Fe(CN)_6]^{3-}$, respectively. Taking into account that the water coordination sphere of both anions makes them bigger, and that the average pore size of the SBA-15 micropores is in the range of 10-12 Å, it can be concluded that the high activity of the SBA-15 supported photocatalysts is due to diffusional restrictions on the

porous structure that prevent the access of iron complexes to the TiO_2 surface, avoiding the deactivation process. This molecular sieve effect introduced by the microporosity of the SBA-15 walls also explains the results obtained with increasing TiO_2 loading, assuming that the reduction of the distance that chemicals must diffuse into the porous structure makes easier the access of the iron complexes to the TiO_2 surface. Concerning the catalyst supported on non-structured silica, its open structure leads to minor differences in the mass transport rate values of CN^- and $[Fe(CN)_6]^{3-}$, producing an intermediate deactivation between that obtained with Degussa P25 and with TiO_2/SBA-15 materials.

5. Conclusions

The photolytic degradation of hexacyanoferrate (II) and (III) aqueous solutions takes place through a progressive cyanide ligand substitution by water molecules, releasing free cyanide species to the medium. Homogeneous oxidation to cyanate is produced only in the ferricyanide degradation, due to the possibility of reduction of pentacyanoferrate (III) species.

Regarding the photocatalytic degradation using TiO_2, an initial step of homogeneous photolysis is also observed, but in this case oxidation of free cyanides to cyanate species can be produced also through the heterogeneous processes taking place on the semiconductor surface. However, the use of bare TiO_2 leads to poor results, due to the existence of a deactivating phenomenon induced by the presence of the iron complexes. In contrast, the use of supported photocatalyst yields better results, partially avoiding the deactivation process due to the adsorption of the iron ions on the silica surface.

Finally, it is important to point out that the use of SBA-15 silica as support leads to a cyanide conversion several times higher than the obtained with Degussa P25 TiO_2. These results have been explained in terms of the molecular sieve effect introduced by the microporosity of the SBA-15 walls, allowing the access of free cyanides to the TiO_2 particles present in the mesoporous channels while iron complexes remain outside of the porous structure.

Acknowledgements

The authors thank “Consejería de Educación, Comunidad de Madrid” for the financial support of this research through the project “Contrato-Programa Grupos Estratégicos de Investigación” and “Ministerio de Ciencia y Tecnología” through the project PPQ2000-1287.

References

1. P. Nielsen, B. Dresow, R. Fischer, H.C. Heinrich, Arch. Toxicol. 64 (1990) 420.

2. N.S. Shifrin, B.D. Beck, T.D. Gauthier, S. D. Chapnick, G. Goodman, Regul. Toxicol. Pharmacol. 23 (1996) 106.

3. L. S. Clescerl, A. E. Greenberg, A. D. Eaton (Ed.), Standard Methods for the Examination of Water and Wastewater, United Book Press, Inc., Baltimore, Maryland, United States, 1998, p. 4.

4. P. Kjeldsen, Water Air Soil Poll. 115 (1999) 279.

5. M.W. Fuller, K.-M.F. Le Brocq, E. Leslie, I.R. Wilson, Aust. J. Chem. 39 (1986) 1411.

6. M. Shirom, G. Stein, J. Chem. Phys. 55 (1971) 3372; *ibid* 55 (1971) 3379.

7. J.C.L. Meeussen, M.G. Keizer, W.H. Van Reimsdijk, V. De Haan, Environ. Sci. Technol. 26 (1992) 1832.

8. E.H. Marsman, J.J.M Appelman, in W.J. van den Brink, R. Bosman, F. Arendt, (Ed.), Contaminated Soil'95, Kluwer Academic Publishers, Dordrecht, Netherlands, 1995, p. 1295.

9. Cyano Compounds, Inorganic in Ullman's encyclopedia of industrial chemistry, 6th edition, Wiley-VCH, Weinheim, Germany, 1998.

10. C.A. Young, T.S Jordan, Cyanide remediation: Current and past technologies, in Proc. 10th Conference on Hazardous Waste Research, Kansas State University, Manhattan, Kansas. May 23-24, 1995.

11. V. Augugliaro, V. Loddo, G. Marcì, L. Palmisano, M.J. López-Muñoz, J. Catal. 166 (1997) 272.

12. T.L. Rose, C. Nanjundiah, J. Phys. Chem. 89 (1985) 3766.

13. S.N. Frank, A.J. Bard, J. Amer. Chem. Soc. 99 (1977) 303.

14. V. Augugliaro, E. García-López, V. Loddo, G. Marcì, L. Palmisano, Adv. Environm. Res. 3 (1999) 179.

15. W.S. Rader, L. Solujic, E.B. Milosavljevic, J.L. Hendrix, Environ. Sci. Technol. 27 (1993) 1875..

16. J. Aguado, R. van Grieken, M.J. López-Muñoz, J. Marugán, Catal. Today 75 (2002) 95.

17. R. van Grieken, J. Aguado, M.J. López-Muñoz, J. Marugán, J. Photochem. Photobiol. A: Chem. 148 (2002) 315.

18. D. Zhao, J. Feng, Q. Huo, N. Melosh, G.H. Fredrickson, B.F. Chmelka, G.D. Stucky, Science 279 (1998) 548.

19. ISO 7766-1:1993 Part 1: Determination of hexacyanoferrate (II) and hexacyanoferrate (III) by spectrometry.

20. G. Emschwiller, J. Legros, Compt. Rend. 261 (1965) 1535.

21. H. Kunkely, A. Vogler, J. Photochem. Photobiol A: Chem. 114 (1998) 197.

22. Z. Stasicka, E. Wasiwlewska, Coord. Chem. Rev. 159 (1997) 271.

23. D.C. Harris, Quantitative Chemical Analysis, 6th edition, W.H. Freeman, Houndmills, England, 2002.

24. J.L. González, M.A. Herraez, S. Rodríguez, J. Col. Interf. Sci. 88(2) (1982) 313.

25. M.A. Anderson, M.H. Palm-Gennen, P.N. renard, C. Defosse and P.G. Rouxhet, J. Col. Interf. Sci. 102(2) (1984) 328.

26. M. Kruk, M. Jaroniec, C.H. Ko, R. Ryoo, Chem. Mater. 12 (2000) 1961.

27. R. van Grieken, G. Calleja, G.D. Stucky, J.A. Melero, R.A. García, J. Iglesias, Langmuir 19 (2003) 3966.